Higher Order Scattering Estimation for PET

Milán Magdics, László Szirmay-Kalos, Balázs Tóth, Balázs Csébfalvi, Tamás Bükki

***Abstract*—The solution of the particle transport problem, which is the core part of tomography reconstruction, is mathematically equivalent to the evaluation of a Neumann series of increasing dimensional integrals, where the first term represents the direct contribution, the second the single scatter contribution, the third the double scattering etc. High dimensional integrals are computationally very expensive, thus this infinite series is truncated after a few (typically after the first or second) terms, which underestimates particle transport results, thus overestimating the radiotracer density in the reconstruction. This paper presents a simple approximate method to improve the accuracy of scatter computation in positron emission tomography without increasing the computation time. We exploit the facts that higher order scattering is a low frequency phenomenon and the Compton effect is strongly forward scattering in 100–511 keV range. Analyzing the integrals of the particle transfer, we come to the conclusion that the directly not evaluated terms of the Neumann seres can approximately be incorporated by the modification of the scattering cross section while the highest considered term is calculated. The proposed model is built into the Teratomo™ system.**

I. Introduction

The solution of the particle transport problem requires the identification of all possible photon paths of arbitrary lengths that can connect the source positions to the detectors, and the integration of the contribution of these paths. The integral should consider all points of the detectors and source locations, as well as all possible scattering points, thus the solution can be expressed as an infinite Neumann series of increasing dimensional integrals, where the first term describes the direct contribution when gamma photons do not scatter in the measured object, the second term the single scattering contribution when one scattering event happens, the third term double scattering, etc. Practical attenuation only methods truncate scatter this infinite Neumann series after the first term, single scatter methods truncate at the second term [13], [1], [4], and double scattering approaches after the third term [12]. Computing just limited number of particle–matter interactions means that the result will be underestimated since ignoring higher order terms replaces their positive contribution by zero.

This negative bias can be eliminated by applying Russian roulette [10], which stops particle paths randomly at interaction points [14], but Russian roulette always increases the variance of the estimator, thus it trades bias for noise. The other drawback of Russian roulette is that different paths have different length, which poses efficiency problems to Single Instruction Multiple Data (SIMD) like parallel hardware architectures like the GPU [11], [5]. The contribution of the terms above truncation can also be approximately re-introduced by blurring and scaling of the calculated contribution [2], [16], [17]. However, these methods cannot accurately consider patient specific data and have the added computational cost of filtering.

The method proposed in this paper applies neither blurring nor random path termination. Instead it modifies the material parameters while the last term of the Neumann series is computed to include the contribution of the missing terms.

The paper is organized in the following way. In Section II we quickly review the model of particle–matter interaction, which leads to an integro-differential equation whose solution can be expressed by an infinite Neumann series. Section III presents our method that modifies the scattering cross section while the last term of the Neumann series is computed. We apply this approximation in PET reconstruction in Section IV considering two scenarios. In the first less accurate scenario, an attenuation only approach is improved by approximately compensating scattering effects. In the second, multiple scattering is added to a single scattering algorithm.

II. Particle–matter interaction

To describe particle–matter interaction, we consider how a beam of photons goes through an emitting, absorbing and scattering medium (Figure 1).

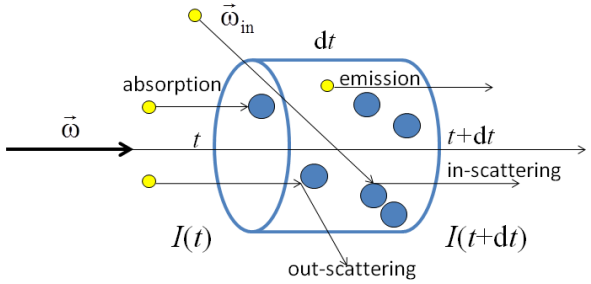

Fig. 1. Modification of the radiant intensity along a ray in emitting, absorbing and scattering media.

Let us consider the radiant intensity I on a linear path of start point $\vec{x}_0$, direction $\vec{\omega}$ and of equation $\vec{x}(t) = \vec{x}_0 + \vec{\omega}t$. Radiant intensity I is modified on differential length $\mathrm{d}t$ by different phenomena:

- **Absorption**: the intensity is decreased when photons collide with the electrons or atomic cores and are absorbed due to the *photoelectric effect*. This effect is proportional to the number of photons entering the path, i.e. the radiant intensity and the probability density of this type

This work has been supported by the TeraTomo project of the National Office for Research and Technology, TÁMOP-4.2.2.B-10/1-2010-0009, OTKA K-101527, and OTKA K-104476, and OTKA K-719922.

M. Magdics, L. Szirmay-Kalos, B. Tóth, and B. Csébfalvi are with Budapest University of Technology and Economics (e-mail: szirmay@iit.bme.hu).

T. Bükki is with Mediso Ltd. (e-mail: Tamas.Bukki@mediso.hu).

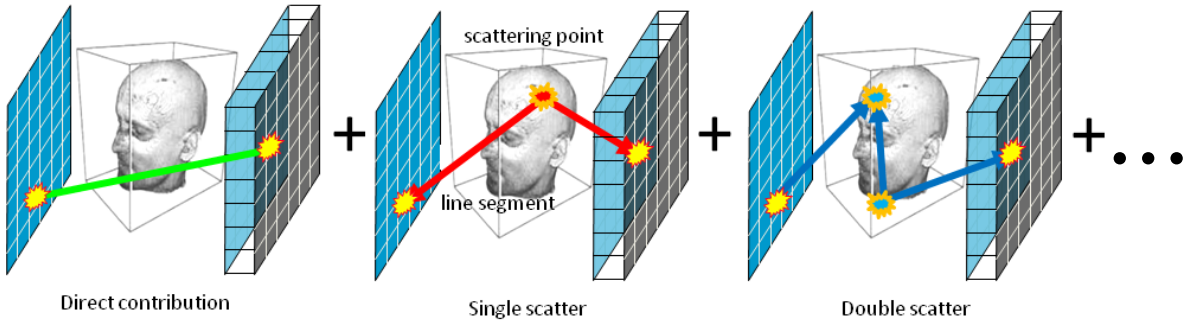

Fig. 2. Expressing the solution of the multiple scattering problem as a Neumann series corresponds to the decomposition of the path space according to the length of the paths.

of collision that is expressed by *absorption cross section* $\sigma_a(\vec{x})$.

- **Out-scattering**: the intensity in this direction is decreased when photons are scattered out from their path. This effect is proportional to the number of photons entering the path and the probability density of such type of collisions, which is described by the *scattering cross section* $\sigma_s(\vec{x})$.
- **Emission**: the intensity may be increased by the photons emitted by the medium. This increase in a unit distance is expressed by the emission density $E(\vec{x})$. We assume that the emission is isotropic, i.e. it is independent of the direction.
- **In-scattering**: photons originally flying in a different direction may be scattered into the considered direction. The expected number of scattered photons from differential solid angle $\mathrm{d}\omega'$ equals to the product of the number of incoming photons and the probability that the photon is scattered in this direction, which is the derivative of the scattering cross section with respect to the scattered direction. The differential cross section can also be expressed as the product of the probability that scattering happened, which is expressed by the scattering cross section, and the conditional probability density that the photon changes its direction from solid angle $\mathrm{d}\omega_{\mathrm{in}}$ to $\vec{\omega}$ provided that scattering happens. The conditional probability density is called the *phase function* $P(\vec{\omega}_{\mathrm{in}}, \vec{\omega})$, which depends on $\vec{\omega}_{\mathrm{in}} \cdot \vec{\omega} = \cos\theta$, where θ is the angle between the incident and scattered directions:

$$\frac{\mathrm{d}\sigma_s}{\mathrm{d}\omega} = \sigma_s(\vec{x}) \cdot P(\vec{\omega}_{\mathrm{in}} \cdot \vec{\omega}).$$

If the photon energy does not change during collision, which happens when the photon collides with an atomic core or a base state, not excited electron, then the scattering is said to be *coherent* or *Rayleigh scattering* (RS). Coherent scattering can be described by the Rayleigh phase function.

$$\frac{\mathrm{d}\sigma_s^{RS}}{\mathrm{d}\omega} \propto 1 + \cos^2\theta.$$

If energy is exchanged between the photon and the electron during scattering, the scattering is said to be *incoherent* or *Compton scattering* (CS). The energy change is defined by the Compton law:

$$\epsilon = \frac{\epsilon_{\mathrm{in}}}{1 + \frac{\epsilon_{\mathrm{in}}}{m_e c^2}(1 - \cos\theta)},$$

where ϵ is the scattered energy, ϵ_{in} is the incident photon energy, m_e is the rest mass of the electron, and c is the speed of light. The differential of the *scattering cross section*, i.e. the probability density that the photon is scattered from direction $\vec{\omega}$ to $\vec{\omega}_{\mathrm{in}}$, is given by the *Klein-Nishina formula* [15]:

$$\frac{\mathrm{d}\sigma_s^{CS}}{\mathrm{d}\omega} \propto \frac{\epsilon}{\epsilon_{\mathrm{in}}} + \left(\frac{\epsilon}{\epsilon_{\mathrm{in}}}\right)^3 - \left(\frac{\epsilon}{\epsilon_{\mathrm{in}}}\right)^2 \sin^2\theta.$$

Taking into account all contributions, intensity $I(\vec{x}, \vec{\omega}, \epsilon)$ of particle flow at energy level ϵ satisfies an integro-differential equation:

$$\vec{\omega} \cdot \vec{\nabla} I(\vec{x}, \vec{\omega}, \epsilon) = -\sigma_t(\vec{x}, \epsilon) I(\vec{x}, \vec{\omega}, \epsilon) + E(\vec{x}, \epsilon) + \int_{\Omega} I(\vec{x}, \vec{\omega}_{\mathrm{in}}, \epsilon_{\mathrm{in}}) \frac{\mathrm{d}\sigma_s(\vec{x}, \vec{\omega}_{\mathrm{in}} \cdot \vec{\omega}, \epsilon_{\mathrm{in}})}{\mathrm{d}\omega_{\mathrm{in}}} \mathrm{d}\omega_{\mathrm{in}}, \quad (1)$$

where $\sigma_t(\vec{x}, \epsilon) = \sigma_a(\vec{x}, \epsilon) + \sigma_s(\vec{x}, \epsilon)$ is the extinction parameter that is the sum of the absorption cross section and the scattering cross section, $E(\vec{x}, \epsilon)$ is the source intensity, Ω is the directional sphere, ϵ_{in} and ϵ are the incident and scattered photon energies, respectively. Scattered photon energy ϵ is equal to incident photon energy ϵ_{in} for coherent scattering. For incoherent scattering, the scattered and incident photon energies are related via scattering angle $\cos\theta = \vec{\omega} \cdot \vec{\omega}_{\mathrm{in}}$ as stated by the Compton law.

In PET [9], source intensity is non zero only at $\epsilon = 511$ keV. Photon energy may drop due to incoherent scattering. As typical detectors are sensitive in the 100–600 keV range, we can ignore photons outside this range. In this energy range and typical materials like water, bone and air, incoherent scattering is far more likely than coherent scattering, thus we can ignore Rayleigh scattering. However, we note that the inclusion of Rayleigh scattering into the model would be straightforward.

According to equation 1, the intensity along a ray is decreased due to absorption and out-scattering. However, photons scattered out show up as a positive contribution in the

in-scattering term in other directions, where they represent a positive contribution. While absorption decreases the intensity along the ray and also the radiation energy globally, out-scattering is a local loss for this ray, but also a positive contribution for other directions, so globally, the number of relevant photons is preserved while their energies may decrease due to the Compton effect.

If the in-scattering integral is ignored, equation 1 becomes a pure linear differential equation

$$\vec{\omega} \cdot \vec{\nabla} I(\vec{x}, \vec{\omega}, \epsilon) = -\sigma_t(\vec{x}, \epsilon) I(\vec{x}, \vec{\omega}, \epsilon) + E(\vec{x}, \epsilon), \qquad (2)$$

which can be solved analytically resulting in

$$I(\vec{x}(t), \vec{\omega}, \epsilon) = T_\epsilon(t_0, t) I(\vec{x}(t_0), \vec{\omega}, \epsilon) + \int_{t_0}^{t} T_\epsilon(s, t) E(\vec{x}(s), \epsilon) \mathrm{d}s, \qquad (3)$$

where

$$T_\epsilon(s, t) = e^{-\int_{t_0}^{t} \sigma_t(\vec{x}(\tau), \epsilon) \mathrm{d}t}$$

is the *attenuation* for photons of energy ϵ between points $\vec{x}(s)$ and $\vec{x}(t)$.

The solution obtained without the in-scattering integral can be used to calculate the full solution if we explicitly sample scattering points, apply this formula for the line segments between the scattering points (Fig. 2), and integrate in the domain of scattering points. Sampling one scattering point between the two detector crystals, we obtain the single scatter contribution, sampling two scattering points, we get the double scatter, etc. Explicitly sampling the scattering points, the contribution of a path is the sum of contributions of a segment multiplied by the attenuation of this and other segments. When segments are considered, we can use the analytic expression of the solution in equation 3 since the in-scattering integral can be ignored because this contribution is taken into account by other higher order terms. This way, the solution of the transport problem is expressed as a sum of contributions of different path lengths. The terms are increasing dimensional integrals since scattering points may be anywhere. The sum of these integrals is called the Neumann series. In practical cases, the infinite Neumann series must be truncated, so the number of considered scattering events is limited.

III. Simplified multiple scattering model for the highest order term

The last really evaluated term of the Neumann series, which represents the highest bounce or longest paths, can be computed in two different ways (Fig. 3):

- We use the same absorption and scattering cross section in the last term as in others, and ignore the higher terms of the Neumann series, which is an *underestimation* because we loose out-scattered photons that may contribute to in-scattering of higher and therefore not computed terms.
- We ignore out-scattering while the last considered term is calculated since this would be the in-scattering of even higher order bounces, which are ignored, thus the energy balance is better maintained if out-scattering on this level is also ignored. This approach leads to a global *overestimation* because allowing neither out-scattering nor in-scattering corresponds to the assumption that scattered photons are never lost by the system, which is not true in reality. This approach replaces scattered paths by shorter line segment, so absorption or dropping the energy below the energy window is less likely. If Compton scattering is considered, changing the photon direction results in an energy drop, which makes absorption even more likely, which even further increases the gap between the contribution of scattered and linear paths. By "global overestimation" we mean that ignoring scattering may decrease the contribution to detectors that can be reached mainly by scattered paths, but increases the linearly reachable path by a larger extent.

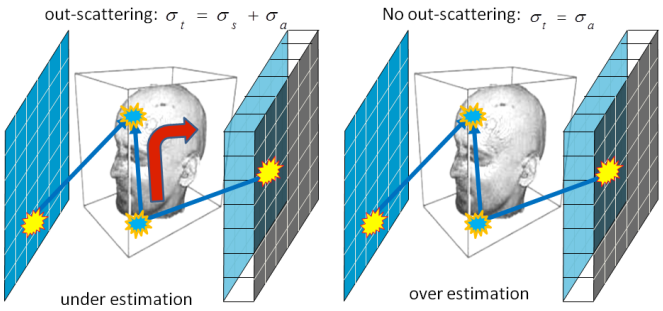

Fig. 3. While computing the highest order term, replacing the extinction coefficient by the absorption cross section and by the sum of the absorption and scattering cross sections results in an overestimation and an underestimation, respectively.

In this paper we propose a simple trick to approximate the true value between the underestimation and overestimation. The approximation is based on the recognition that both the underestimating and the overestimating cases correspond to the modification of volume properties in equation 1, and are members of a much wider family, which also includes cases in between the extreme ones. The two extreme approximations correspond to replacing the Klein-Nishina differential cross section by Dirac-delta $\delta(\vec{\omega} - \vec{\omega}_{\mathrm{in}})$ scaled by zero or by the scattering cross section, respectively. In-betweening approximations can be obtained by additionally scaling of the Dirac-delta by parameter λ that is between 0 and 1, which leads to our simplified scattering model:

$$\frac{\mathrm{d}\sigma_s(\vec{x}, \vec{\omega}_{\mathrm{in}} \cdot \vec{\omega}, \epsilon_{\mathrm{in}})}{\mathrm{d}\omega_{\mathrm{in}}} \approx \lambda \sigma_s(\vec{x}, \epsilon) \delta(\vec{\omega} - \vec{\omega}_{\mathrm{in}})$$

where $\epsilon_{\mathrm{in}} = \epsilon$ since the Compton effect does not change the photon energy when the direction is not altered. We emphasize that this simplified model is used only when the line integrals of the highest considered term are evaluated, in all other cases, the original Klein-Nishina formula is applied.

Substituting the simplified model into equation 1, we obtain

$$\vec{\omega} \cdot \vec{\nabla} I(\vec{x}, \vec{\omega}) = -(\sigma_a(\vec{x}) + \sigma_s(\vec{x})) I(\vec{x}, \vec{\omega}) + E(\vec{x}) + \lambda \sigma_s(\vec{x}) I(\vec{x}, \vec{\omega}),$$

where functions are evaluated on the same energy level ϵ. The term coming from the in-scattering integral can be interpreted as the modification of the scattering cross section, so we get a

pure differential equation that is similar to equation 2 obtained by ignoring the in-scattering term:

$$\vec{\omega} \cdot \vec{\nabla} I(\vec{x}, \vec{\omega}, \epsilon) = -(\sigma_a(\vec{x}, \epsilon) + \sigma'_s(\vec{x}, \epsilon)) I(\vec{x}, \vec{\omega}, \epsilon) + E(\vec{x}, \epsilon),$$

where $\sigma'_s = (1-\lambda)\sigma_s$. The solution of the differential equation can be expressed in the same form as equation 3 having replaced scattering cross section σ_s by $(1-\lambda)\sigma_s$. The accuracy of this approximation depends on the proper choice of λ and on how strongly the phase function is forward scattering and is similar to a Dirac-delta function. Intuitively, parameter λ expresses the probability that a photon scattered more than the limit caused by the truncation of the Neumann seres gets lost for the system.

We have two options to find an appropriate λ parameter. Based on its probabilistic interpretation, the probability that a photon gets lost due to scattering more times than the considered limit can be determined by an off-line simulation with e.g. GATE [3]. This probability depends on the tomograph geometry, the size of the the object and also on the maximum number of bounces, so several simulation studies are needed for different measurement protocols. The other option is simpler and is based on the geometric evaluation of the tomograph. The details of this approximation is discussed in the next subsection. As we shall demonstrate in the Results Section, the reconstruction quality is not strongly sensitive to the exact choice of parameter λ, so the exact value is not important, and good results can be obtained with rough approximations of λ as well.

A. Determination of parameter λ

The modification of the scattering cross section during the evaluation of the line integrals of the highest simulated bounce requires parameter λ, which determines the probability of scattering when the direction is not significantly changed. The main reasons of the energy loss in a scattering only media is that the photon leaves the system without interacting with the detector ring and that the energy of the photon drops below the minimum value of the energy window (typically 100 keV) due to the Compton effect.

Back-scattering means lost photons since when the direction is reversed once, the photons of the annihilation pair arrive at detector modules that are not in coincidence, so this photon pair is ignored by the electronics. Multiple direction reverses are unlikely and reduce the photon energy significantly (one full back-scattering reduces the energy of an 511 keV photon to the third of its original energy and two full back-scattering events to the fifth), thus these photons will be ignored since their energy is outside of the energy window.

Considering forward scattering only, a conservative approach to λ would be the computation of the probability that the photon hits the same detector crystal after scattering as it would hit traveling a linear path. Clearly, such scattering events are not even recognized by the measurement system. This probability is equal to the integral of the phase function over the solid angle subtended by the detector crystal surface.

However, this conservative estimation ignores the fact that the scatter component already has low frequency characteristics, so the beam that is analyzed can be assumed to be wider.

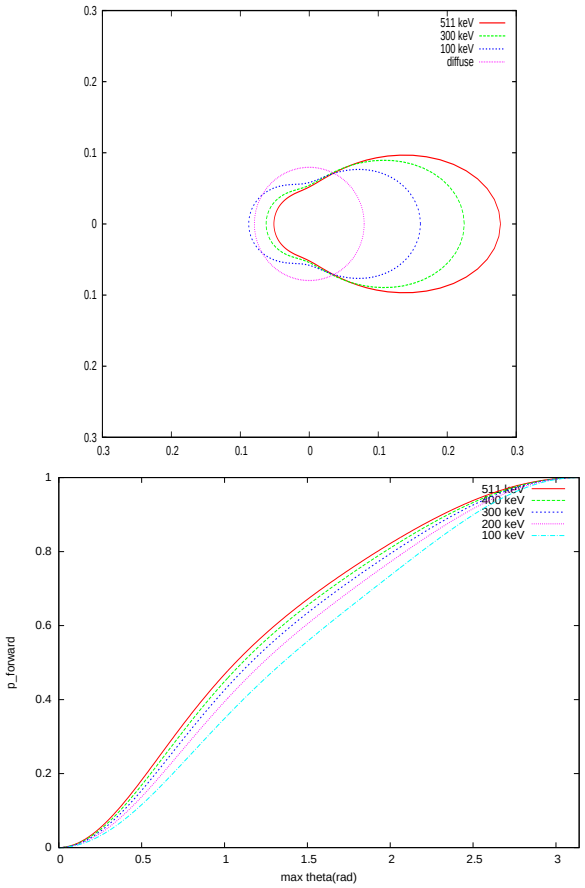

Fig. 4. Klein-Nishina phase function assuming different incident photon energies (upper image). For comparison, we also show the phase function of isotropic diffuse materials. The forward scattering probability with respect to the allowed maximum scattering angle in radian (lower image).

So, even if a photon changes its direction so significantly that it arrives at a different detector crystal, which results in a contribution drop for this LOR, we can assume that other paths parallel to the current one can be handled similarly, so their loss is a positive contribution in the considered LOR. In a wider homogeneous beam, changing photon directions compensates each other. So, the solid angle in which the phase function needs to be integrated can be wider, and can be increased up to the solid angle in which the detector modules being in coincidence relation can be seen. In Mediso's AnyScan PET/CT geometry, the maximum perturbation angle of a line that ensures that the intersected modules will be the same is about 30–45 degrees (0.5–0.6 radians).

Fig. 4 shows the integral of the phase function of Compton scattering in solid angles defined by the maximum scattering angle. Note that in the 0.5–0.6 radian range, the integral is between 0.2–0.3 and is roughly independent of the photon energy, thus the lambda parameter should be selected around this value.

IV. Application in the Scatter Compensation for PET

If we consider photon scattering, the path of the photon pair will be a *polyline* containing the emission point somewhere

inside one of its line segments (Fig. 2). This polyline is defined by the scattering points where one of the photons changed its direction in addition to the detector hit points. The values measured by detector pairs will then be the total contribution, i.e. the integral of such polyline paths of arbitrary length. Higher order bounces include more integrals according to the possible scattering points. In order to save the increased computation time, we propose to accurately compute only the direct contribution and/or single scattering. When these are evaluated, we use the idea of incorporating the not computed higher order bounces (i.e. double, triple etc. scattering) by modifying the scattering cross section.

Our proposed method should be used when the longest paths are computed. We consider two reconstruction scenarios based on the definition of the maximum length:

- **Attenuation only** reconstruction completely ignores scattering and computes only the direct contribution, i.e. photon paths that connect crystals by line segments. In this extreme case, our proposed modification should work on the level of direct contribution computation, and the contribution of ignored scattered paths is approximately reintroduced by the modification of the scattering cross section while attenuation of the direct contribution is computed.
- **Single scatter compensation** can be further improved by including the energy of multiple scattering in the contribution of single scattered paths.

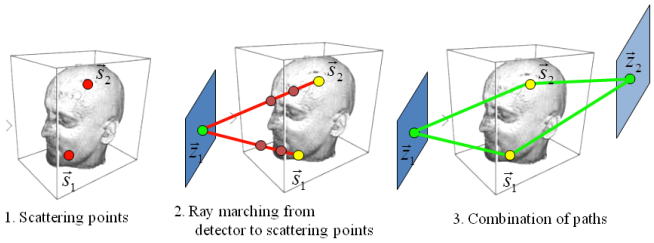

Fig. 5. The basis of our multiple scattering compensation method is a modified Watson algorithm that is responsible for single scatter compensation.

The single scattered contribution to a LOR will be the integral of path contributions, which is computed by the Watson's method [13] with the following modifications:

1) Instead of computing the polyline contribution separately for each LOR, the process is decomposed to three phases to allow the reuse of line integrals in multiple LORs. In the first phase, N_{scatter} scattering points are sampled globally, which will be used in the quadratures of all LORs. In the second phase, each detector crystal is connected to each of the scattering points, and along these line segments the line integrals of the total activity, total attenuation due to the photoelectric effect and total out-scattering due to the Compton effect are computed. Absorbtion and scattering cross sections depend on the energy of gamma photons, which is not available yet, thus these line integrals are temporarily computed assuming 511 keV photons. In the third phase, the line segments sharing a scattering point are paired, resulting in N_{scatter} polylines in each LOR. When a polyline is formed, the scattering angle and thus the Compton formula can be evaluated. The total out-scattering and attenuation are corrected according to the ratios of the real photon energy and 511 keV energy [6].
2) Instead of uniform sampling, global scattering points are sampled from a probability density that mimics the scattering cross section, and the contribution is simultaneously divided with this density since this reduces the variance of the Monte Carlo quadrature according to *importance sampling*.

Note that this three-phase approach significantly reduces the number of line integrals to be computed as it reuses results obtained in the first two phases. As a side effect of reusing samples, the approximation errors in different LORs are correlated, thus the reconstruction will be free of dot noise typical in other Monte Carlo algorithms.

V. Results

The method is demonstrated with simulating Mediso's AnyScan PET/CT system [8] with GATE [3] for the NEMA NU2-2007 human IQ phantom. AnyScan has 24 detector modules consisting of 27×38 crystals detectors of $3.9^2 \times 20$ mm^3. For the AnyScan PET/CT, the optimal λ is 0.2–0.3 according to the geometric considerations of Section III-A. The proposed method can be used together with zero (i.e. attenuation compensation), first, second, etc. order scattering compensation at no additional cost. We should just modify the scattering cross section while the highest bounce is calculated.

We consider the two discussed scenarios. In the first one, we extend an attenuation only approach that calculates no scattering to approximately consider scattering effects. In the second scenario, we start with a single scattering compensation algorithm and improve it to include multiple scattering effects.

A. Adding scattering compensation to attenuation compensation in PET

If we wish to approximately include single and multiple scattering without computing these factors, then the scattering cross section should be modified during the attenuation calculation as

$$\sigma_s' = \sigma_s(1 - \lambda)$$

where λ is a system parameter depending on the solid angle in which the detectors are seen.

Figure 6 shows the L2 error curves of the reconstruction with attenuation simulation while the classical approach is used and when the scattering cross section is modified. For comparison, we also included the error curves when single scattering is simulated, and when multiple scattering is also approximated by modifying the scattering cross section during single scatter simulation. The coronal and transverse slices of the reconstructed data are shown by Figure 7.

Observe that the simple modification of the scattering cross section during attenuation calculating significantly improved the L2 error curves reducing and also the reconstruction images and made similar to those of obtained with a single scatter compensation, however, it cannot reach that quality.

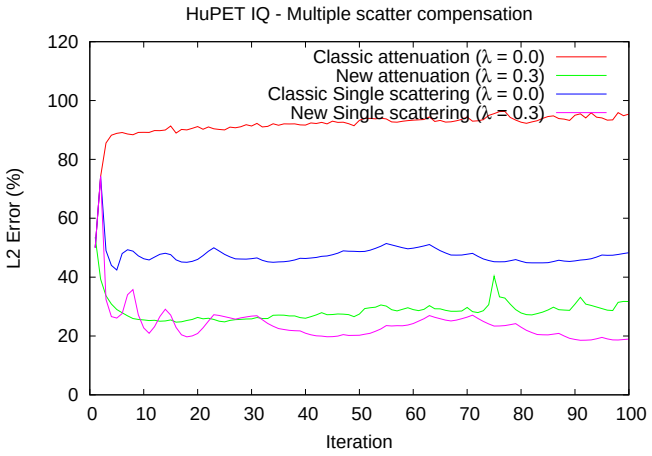

Fig. 6. L2 error curves of the reconstruction of the human IQ phantom while attenuation only simulation is executed in forward projection and also in back projection. In this phase, we control the scattering cross section with the λ parameter. Setting it to zero, we get the case of classical attenuation simulation back. Setting $\lambda = 0.3$ represents our new method. For comparison, we also included the L2 curves when single scattering is explicitly calculated.

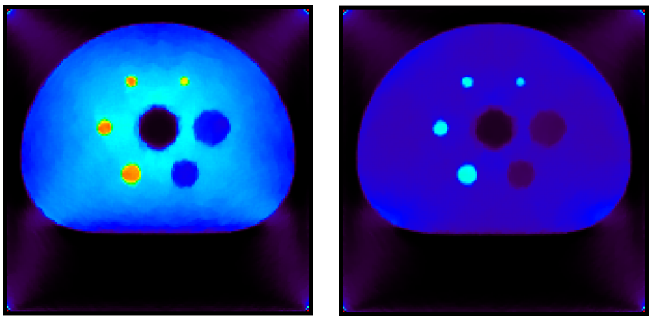

Classic Attenuation Only
$\lambda = 0$

New Attenuation Only
$\lambda = 0.3$

Fig. 7. Transverse slices of the Attenuation only reconstruction of the simulated IQ phantom.

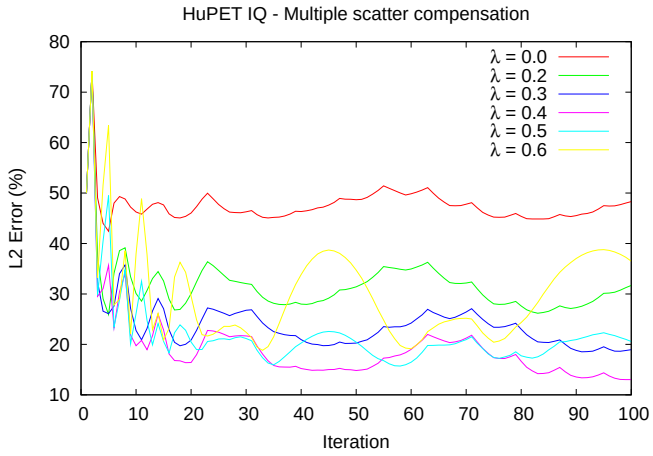

Fig. 8. L2 error curves of the Single scatter compensation reconstruction of the IQ phantom while the λ parameter is selected in the 0.2–0.5 range. The wavy error curves are due to the fact that scattering is simulated just in every third iteration step to reduce computation time.

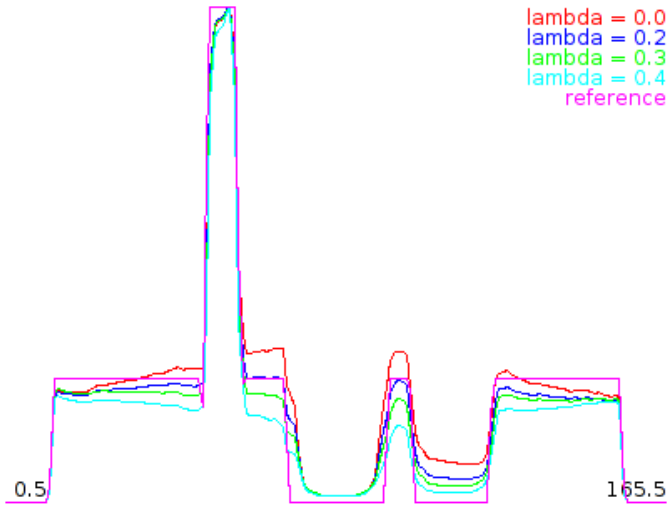

Fig. 10. Line profiles of the Single scatter reconstruction of the measured IQ phantom while the λ parameter is selected in the 0.0–0.5 range.

B. Adding multiple scattering compensation to single scattering methods

Here we present the improvement of the single scatter compensation of the Teratomo^{TM} system [7].

Fig. 9 shows the transaxial slices of the reconstruction of the human IQ phantom, Fig. 10 depicts line profiles, and Fig. 11 the NEMA evaluation. When λ is small, the results are similar to that of classical single scatter compensation where the ignored energy causes an overestimation of the activity in the center of the phantom. Increasing λ this artifact disappears and the homogeneous region is reconstructed with constant activity. However, increasing λ beyond the reasonable range, the missing energy will be overcompensated, which shows up as a decreased reconstructed activity around the spine when $\lambda \geq 0.4$. The method is quite robust to the particular selection of λ, an arbitrary value in $[0.2, 0.3]$ would improve the results without this artifact.

Examining the NEMA evaluation, we can observe that contrasts grow with higher λ, and background variability first decrease that start to rapidly increase if $\lambda > 0.4$. The reason is overcompensation, which means that the center of the phantom gets darker than expected.

VI. Conclusion

This paper proposed a simple correction to take into account higher scattering in PET reconstruction. The method corrects the scattering cross section when the highest computed bounce is evaluated, approximately including the contribution of the bounces above this level. As having modified the scattering cross section, the algorithm remains the same, the proposed correction has no computational overhead.

We demonstrated the proposed correction with two scenarios. In the first one, no scattering is directly computed, only the attenuation calculation is modified according to the new proposal. In the second scenario, we improved the accuracy of a single scatter compensation method by approximately

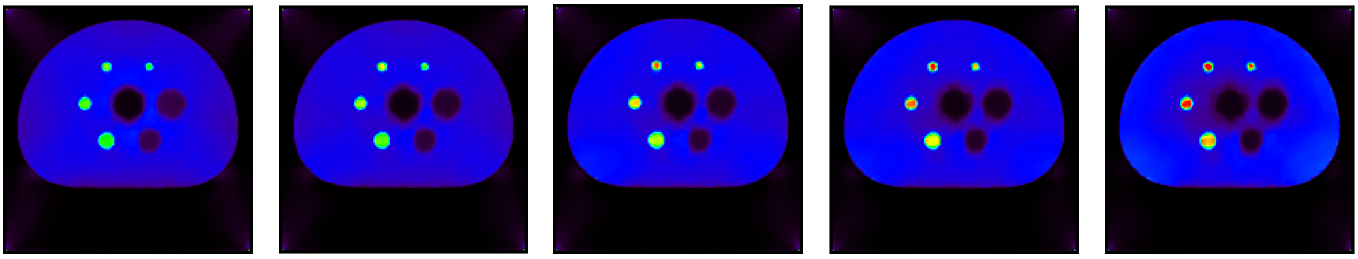

Classic Single Scatter | New Scatter $\lambda = 0.2$ | New Scatter $\lambda = 0.3$ | New Scatter $\lambda = 0.4$ | New Scatter $\lambda = 0.5$

Fig. 9. Transverse slices and line profiles of single scatter compensation reconstruction of the human IQ phantom with different λ parameters.

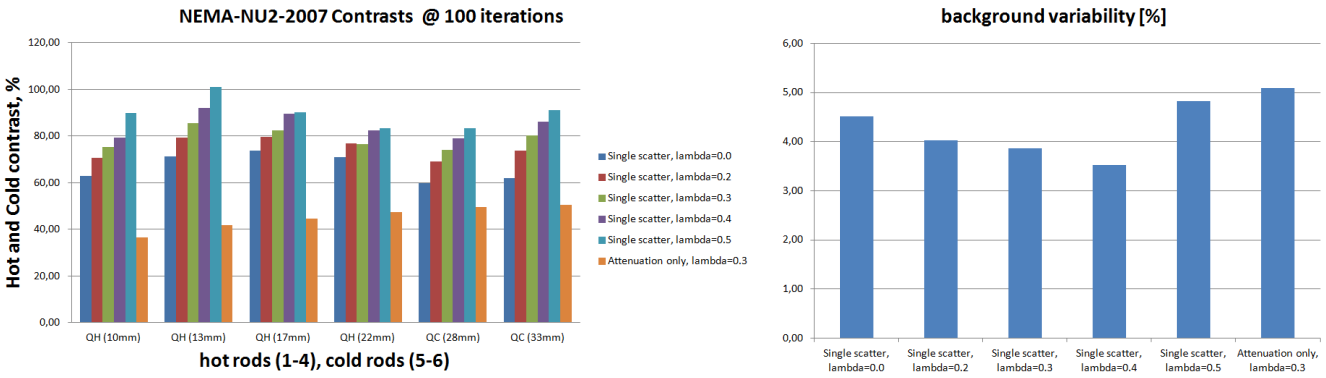

Fig. 11. Contrast factors and background variability of the IQ phantom according to the NEMA standard. Note that increasing parameter λ, contrasts also increase, while the background variability first improves then starts degrading.

include multiple scattering contribution. In both cases significantly lower L2 error can be obtained, contrast ratios and background variability are also improved. The correction is based on a single parameter that describes the probability that a photon gets lost for the total system because of scattering. We discussed a simple approximation to obtain this parameter and showed that reconstruction quality can be increased even with roughly approximated parameter values.

References

[1] Werling A., Bublitz O., Doll J., and et al. Fast implementation of the single scatter simulation algorithm and its use in iterative image reconstruction of PET data. *Physics in Medicine and Biology*, 47:2947–60, 2002.

[2] Lecomte R. Bentourkia M. Energy dependence of nonstationary scatter subtraction-restoration in high resolution PET. *IEEE Transactions on Medical Imaging*, 18:66–73, 1999.

[3] S. Jan and et al. GATE: A simulation toolkit for PET and SPECT. *Physics in Medicine and Biology*, 49(19):4543–4561, 2004. http://www.opengatecollaboration.org.

[4] K. S. Kim and J. C. Ye. Fully 3D iterative scatter-corrected OSEM for HRRT PET using GPU. *Physics in Medicine and Biology*, 56:4991–5009, 2011.

[5] L. Szécsi L. Szirmay-Kalos. General purpose computing on graphics processing units. In A. Iványi, editor, *Algorithms of Informatics*, pages 1451–1495. MondArt Kiadó, Budapest, 2010. http://sirkan.iit.bme.hu/szirmay/gpgpu.pdf.

[6] M. Magdics, L. Szirmay-Kalos, B. Tóth, Á. Csendesi, and A. Penzov. Scatter estimation for PET reconstruction. In *Proceedings of the 7th international conference on Numerical methods and applications*, NMA'10, pages 77–86, Berlin, Heidelberg, 2011. Springer-Verlag.

[7] M. Magdics, L. Szirmay-Kalos, B. Tóth, D. Légrády, Á. Cserkaszky, L. Balkay, B. Domonkos, D. Völgyes, G. Patay, P. Major, J. Lantos, and T. Bükki. Performance Evaluation of Scatter Modeling of the GPU-based "Tera-Tomo" 3D PET Reconstruction. In *IEEE Nuclear Science Symposium and Medical Imaging*, pages 4086–4088, 2011.

[8] Mediso. Anyscan PET/CT. http://www.mediso.com/products.php?fid=1,9&pid=73.

[9] A. J. Reader and H. Zaidi. Advances in PET image reconstruction. *PET Clinics*, 2(2):173–190, 2007.

[10] L. Szirmay-Kalos. *Monte-Carlo Methods in Global Illumination — Photo-realistic Rendering with Randomization*. VDM, Verlag Dr. Müller, Saarbrücken, 2008.

[11] L. Szirmay-Kalos, B. Tóth, and M. Magdics. *GPU Computing Gems*, chapter Monte Carlo Photon Transport on the GPU, pages 234–255. Morgan Kaufmann Publishers, 2010.

[12] C. Tsoumpas, P. Aguiar, D. Ros, N. Dikaios, and K. Thielemans. Ieee nuclear science symposium conference record. In *Full 3D Concerence*, pages 1619–24, 2005.

[13] C.C. Watson, D. Newport, and M.E. Casey. *Three-Dimensional Image Reconstruction in Radiation and Nuclear Medicine*, chapter A single scattering simulation technique for scatter correction in 3D PET, pages 255–268. Kluwer Academic Publishers, 1996.

[14] A. Wirth, A. Cserkaszky, B. Kári, D. Legrády, S. Fehér, S. Czifrus, and B. Domonkos. Implementation of 3D Monte Carlo PET reconstruction algorithm on GPU. In *Nuclear Science Symposium Conference Record (NSS/MIC), 2009 IEEE*, pages 4106–4109, 24 2009-nov. 1 2009.

[15] C. N. Yang. The Klein-Nishina formula & quantum electrodynamics. *Lect. Notes Phys.*, 746:393–397, 2008.

[16] H. Zaidi and K. F. Koral. Scatter modelling and compensation in emission tomography. *Eur. J. Nucl. Med. Mol. I.*, 31:761–782, 2004.

[17] Habib Zaidi and Marie-Louise Montandon. Scatter compensation techniques in PET. *PET Clinics*, 2(2):218–234, 2007.